Small Pitch Tilting Spine Optical Fiber Positioners for Massively Parallel Spectroscopy

Rebekah A. Sebok[*a], Finian Ashmead[b], H. Thomas Diehl[b], Parth Gandhi[b], Jingqi Fan[a], Ayla M. Rodriguez[a], Kyler Kuehn[c], Marcelle Soares-Santos[a], Jennifer L. Marshall[d], Luke M. Schmidt[d], Theresa M. Shaw[b], Stephen M. Kent[b], Alex Drlica-Wagner[b]
[a]Department of Physics, University of Michigan, 450 Church St, Ann Arbor, Michigan, USA, 48109
[b]Fermi National Accelerator Laboratory, P.O. Box 500, Batavia, IL, USA, 60510
[c]Lowell Observatory, 1400 W. Mars Hill Rd, Flagstaff, AZ, USA, 86001
[d]Mitchell Institute for Fundamental Physics and Astronomy and Department of Physics and Astronomy, Texas A&M University, College Station, TX 77843-4242, USA

Abstract. Massively-multiplexed spectroscopic surveys rely on precise optical fiber-positioning technology to match the fiber positions in physical space to targets observed on-sky. Several different technologies have been used for such devices, including Tilting Spines, Twirling Posts, and Walking Bugs; each of these has its own advantages and drawbacks in terms of parallelization, pitch, exclusion radius, and other relevant operational factors. Current instruments using Tilting Spines operate with a pitch (that is, the separation between adjacent spines) of approximately 9 mm. Reducing the pitch to 5 mm allows for observations of many more targets in parallel, as well as (potentially) much denser target fields. Here we describe engineering efforts and progress towards reducing the pitch between adjacent Tilting Spines. We conclude with a brief discussion of the impact an instrument with very densely packed fiber positioners would have on massively-multiplexed astronomical observations.

Keywords: fiber positioner, multi-object spectroscopy, fiber spectroscopy.

* rsebok@umich.edu

1 Introduction

Optical imaging projects such as the Sloan Digital Sky Survey,[1] the Kilo-Degree Survey, and the Dark Energy Survey are wide-field surveys with massive datasets[2–4] comprising hundreds of millions of stars and galaxies. The upcoming Legacy Survey of Space and Time will provide a map of billions of objects in the full southern sky. The rich science of these surveys spans astrophysics from objects in solar system, to Milky Way structures, large-scale structure and cosmology in the extra-galactic universe.[5–8] Spectroscopic follow-up of these surveys has created a need for wide-field instruments that can make thousands of measurements in parallel. The current leaders have from 2400 to 5000 FPs on the focal surface.

Early planning within the scientific community acknowledges the priority for spectroscopy: ”a strong R&D effort builds toward the ultimate next-generation wide-field spectroscopic survey Spec-S5, which will study the possible time evolution of dark energy and provide a test of inflation complementary to CMB-S4”.[9] The next generation of wide-field spectroscopic instruments could expect to measure tens of thousands of spectra simultaneously.[10]

1.1 Need for Small Pitch

Instrument technology has evolved since plug-plates, where optical fibers were inserted by hand into pre-drilled holes in a plate that would be mounted on a focal surface, to various sorts of robotic fiber positioners (FPs), which could be individually controlled. These next generation instruments will achieve the improvement in parallelization through decreasing the center-to-center distance (pitch) between FPs. The white paper “Cosmic Visions: Small Projects Portfolio”[11] and the SNOWMass Report on the Cosmic Frontier on Dark Energy and Cosmic Acceleration[12] highlight the need for R&D into decreasing the minimum pitch of FP technologies for precisely this purpose.

1.2 Robotic Fiber Positioner Technologies

There are three conceptually different current FP technologies. “Walking Bugs” are well-represented by the TAIPAN instrument.[13] TAIPAN FPs are called “Starbugs”, where an optical fiber is held in contact with a glass plate using a slight air suction, and uses coaxial piezoelectric tubes to perform a lift and step motion that can “walk” the fiber anywhere on the plate (of course, the focal surface).

There are a couple representative “Twirling Posts” including the “Cobra” on the Subaru Telescope’s Prime Focus spectrograph (PSF),[14] which positions the tip of an optical fiber on a rotating arm, which is in turn mounted on a rotating post ("thus Twirling Post"). The rotations are accomplished using piezo "wobbly" motors. Similarly, the DESI instrument[15] holds an optical fiber at the top of a rotating arm on a rotating post, where the rotations are accomplished using two tiny brushless gear motors.

The original "Tilting Spine" FP was designed and built for FMOS.[16] Most generally, a unit Tilting Spine FP consists of a thin tube that has the optical fiber inside of it starting at the focal surface end. The tube is tilted by some mechanism, generally a piezo-electric device, so that the tip of the optical fiber is at the desired location. We describe our simple version below, in Sec. 2. European Southern Observatory is receiving a 2^{nd} generation Tilting Spine instrument called 4MOST.[17]

The Walking Bugs, Twirling Posts, and Tilting Spines each have advantages and disadvantages flowing from the scientific requirements of the project to technical specifications such as details of the incoming optical beam, the number and separation of targets that need to be observed simultaneously, the amount of time available for observations, etc. Table 1 lists a few instruments of each kind, including some (previously noted) that were built,[13–17] some that never were,[18] and some that want-to-be.[19–22]

2 A sub-6 mm Pitch Tilting Spine FP

The fiber positioner design we used was based on that of the MOHAWK,[18] possibly the simplest Tilting Design possible. We elected to make it using off-the-shelf materials and components where possible and exceptions are noted below. Fig. 1 shows photographs of the spine assembly and the piezo-tube assembly.

For the Tilting Spine assembly, we used a 30.5 cm-long 1.5 mm O.D. (0.7 mm I.D) carbon fiber

Table 1 Some representative instruments using FPs. * indicates conceived but not built. ** indicates possible future projects.

Telescope	Instrument	FP Technology	No. FP	Pitch
Subaru (8m)	FMOS-Echidna	Tilting Spine	400	7.5 mm
UKST (1.2m)	TAIPAN	Walking Bug	150-300	∼10 mm
Mayall (4m)	DESI	Twirling Post	5000	11 mm
Subaru (8m)	PFS	Twirling Post	2394	8 mm
VISTA (4.1m)	4MOST	Tilting Spine	2400	9.5 mm
Blanco (4m)	MOHAWK*	Tilting Spine	4000	7 mm
Mayall (4m)	DESI II**	Twirling Post	11250	6.1 mm
FOBOS (10m)	Keck II**	Walking Bug	1800	∼10 mm
MSE (11.25m)	Sphinx**	Tilting Spine	4332	7.7 mm
Magellan-like (6.5m)	MegaMapper**	Twirling Post	26100	6.1 mm
SpecTel (11.4m)	Spec-S5**	Twirling Post	15000	11 mm
TBD	Spec-S5**	TBD	60000	5 mm

tube. On one end of the tube was glued a 544 phosphor bronze counterweight of 3/16” diameter and 35 mm length, with a 5 mm diameter 440C S.S. ball immediately below. Of course, we had to drill 1.5 mm diameter holes in the ball and CW. For some of the final assemblies, an 0.7 mm diameter, 10.5 mm long, custom zirconia ferrule with an 128 μm diameter hole held a meters-long Thorlabs FG105LCA (multiclad) optical fiber, polished, at the working end of the spine, though for others early-on we omitted the optical fiber. Polishing was done using ThorLabs polishing paper of 4 successively finer grits from 5 microns to 0.3 microns on a glass polishing plate and with a custom, hand-held polishing disc. The polished end of the fiber was inspected using an FS201 fiber inspection scope from the same company. Fig. 2 shows details of the ferrule-to-fiber-to-spine assembly. The full spine assembly consists of five parts held together using epoxy or cyano-acrylate glue. This unit design has a maximum diameter of 5 mm, and total mass of ∼10 grams.

The piezo assembly comprised a ring magnet glued to a piezo-electric tube, which was glued to a simple circuit board. Component alignment was achieved using simple small Teflon jigs. The

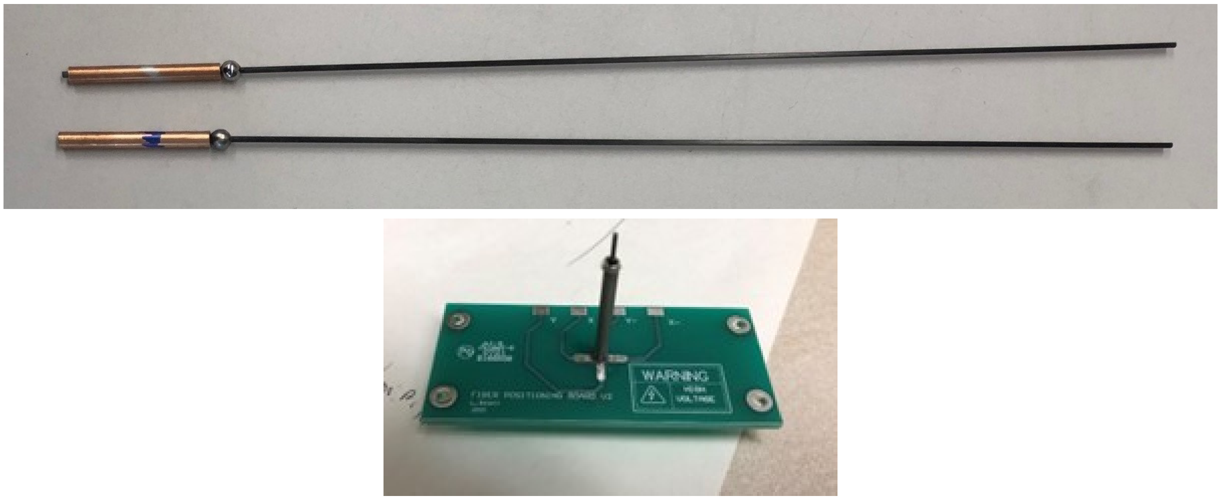

Fig 1 This shows two Tilting Spine assemblies (upper), with bronze counterweight, steel ball, and carbon fiber tube, but without the optical fiber. Below that is the piezo assembly soldered to the circuit board. The piece sticking up through the center of the piezo tube is part of the assembly tooling and is removed for use on the test stand.

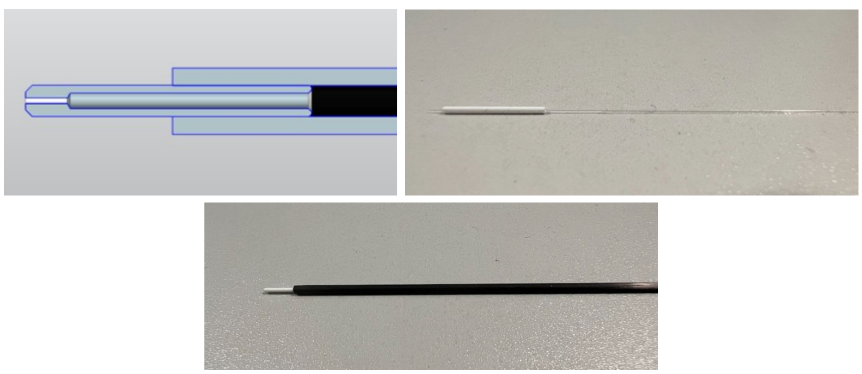

Fig 2 Detail of the ferrule, fiber, and spine assembly. The upper-left picture shows a engineering cartoon. The optical fiber diameter is tiny, even compared to the ferrule. The upper-right is a photo of a ferrule with an optical fiber glued into it. The lower photo shows the ferrule assembly embedded and glued into a carbon fiber tube.

piezoelectric tube was a PT-230.94, a 4-electrode x-y scanner tube from PI (Physik Instrumente) L.P. The N50 Neodymium ring magnets were 4 mm O.D., 3 mm I.D. and 1 mm thick. We found that with our design, the coupling force between the ball and magnet was insufficient with smaller diameter magnets. The simple circuit accommodated the 4 leads of the piezo, and had a hole through it for the carbon fiber tube.

3 Test Stands at Fermilab and University of Michigan

We built two similar test stands, one at Fermilab and another at the University of Michigan. We describe the components and controls software in this section.

3.1 Test Stand Hardware Components

The test stands were similar to each other in that each used the spine & piezo assemblies described in Section 2. The Fermilab-based test stand used a KEYSIGHT EDU33212A 20 MHz Waveform Generator and a PIEZODRIVE TD250-INV voltage amplifier to move the FP. That test stand used a Raspberry Pi4 2GB microcomputer to direct an Arducam Lens Board OV5647 Sensor (a small, inexpensive camera) to take and store photographs of the tip of the spine. The UM-based test stand used BK Precision 4000-series waveform generator with the same voltage amplifier to move the FP. U. Michigan used a 30 frame-per-second Basler ace 2 a2A4096-30umBAS videocamera with a Raspberry Pi SCO123 CGL 16mm tele-photo lens. All of these components were controlled by modest Windows PCs in both locations. Photos of the two test stands are shown in Fig. 3.

3.2 Test Stand Control Software

The controls software were written using PYTHON 3 routines. They were developed individually and then integrated into Tkinter GUI interfaces. A sample GUI is shown in Fig. 4. Each button in the figure initiates an action, which might be a complete function, or might open another GUI. Functions variously controlled the KEYSIGHT waveform generator via PYVISA to move the spine a given number of steps at a given pulse amplitude, direct the Raspberry Pi4 microcomputer, find the position of the tip of the spine in an image using the open-source PYTHON 3 module cv2.HoughCircles (see Fig. 5, calibrate the step size vs. waveform generator voltage, go to the

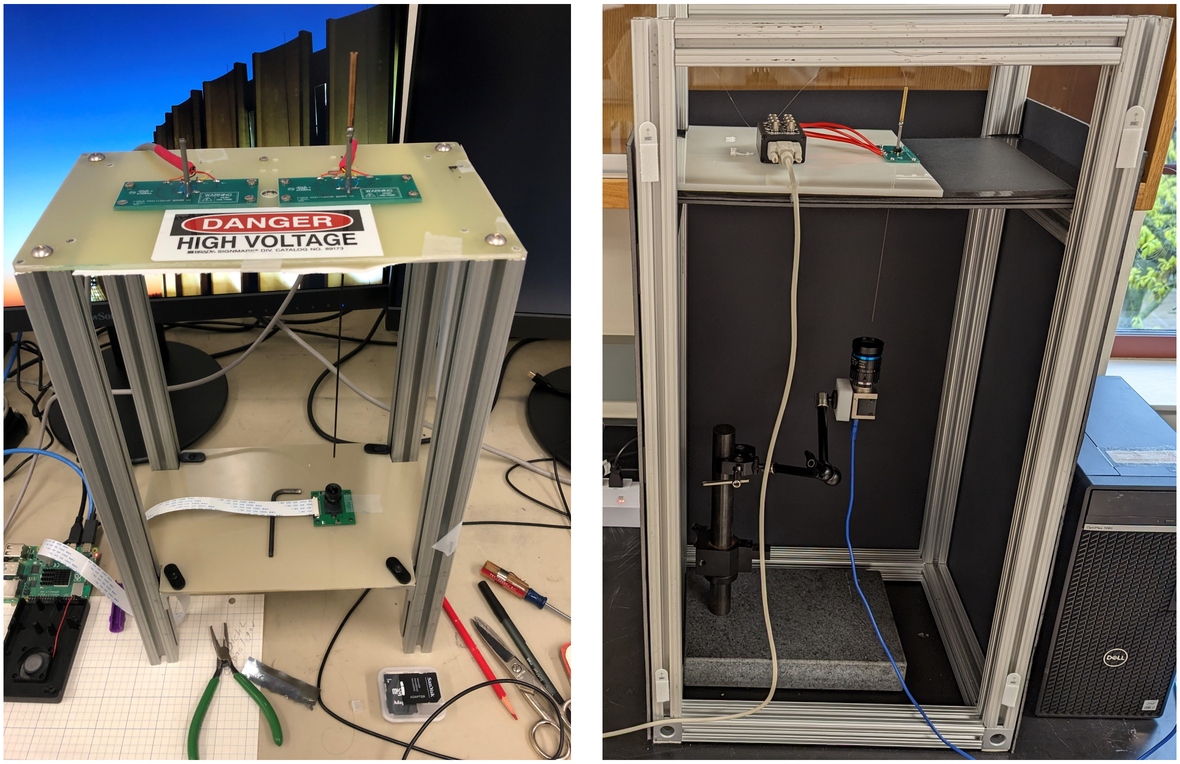

Fig 3 Test stand mechanical setups at Fermilab (LHS) and U. Michigan (RHS).

no-tile “Home” position, and go to any other desired location within a certain number of iterations and to a certain accuracy. Other functions not shown on this figure included finding the maximum tilt in any given direction, fitting a circle to the resulting data point (to find the ”patrol radius”), and defining the home position, among others.

Incidentally, we found that the choice of PYTHON as the control language made the task of code development very accessible, productive, and successful for the LDRD team.

4 Movement Algorithm and Results

With this equipment we were able to move the spine. The minimum voltage required to move the FP was 1V (25V) from the waveform generator (voltage amplifier). Our first experiments were to establish movement distance versus peak voltage. Fig. 6 shows that the movements are linear with the number of sawtooth waveforms applied (“ticks”) and that distance of the movement

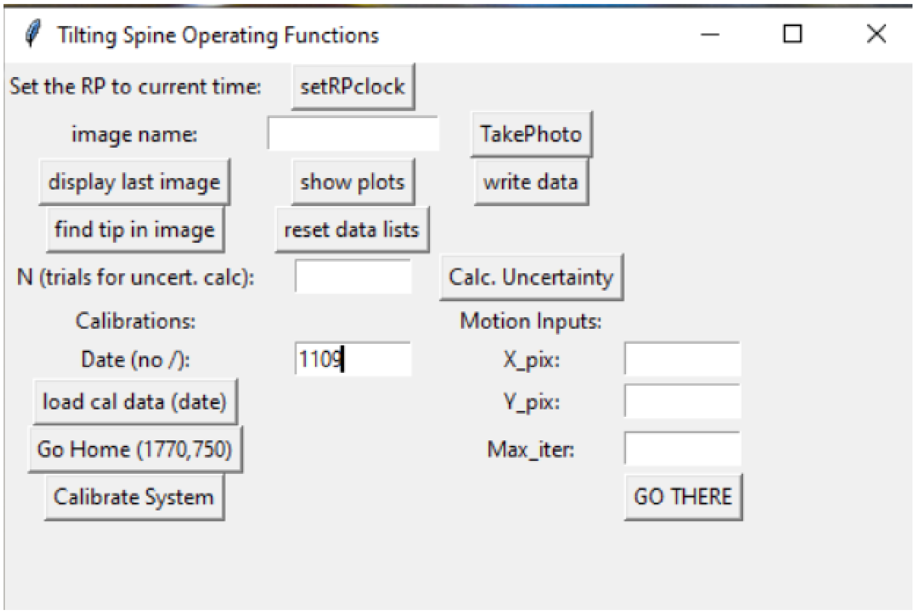

Fig 4 Tilting Spine control GUI showing many of the functions that we developed. Each button initiates an action.

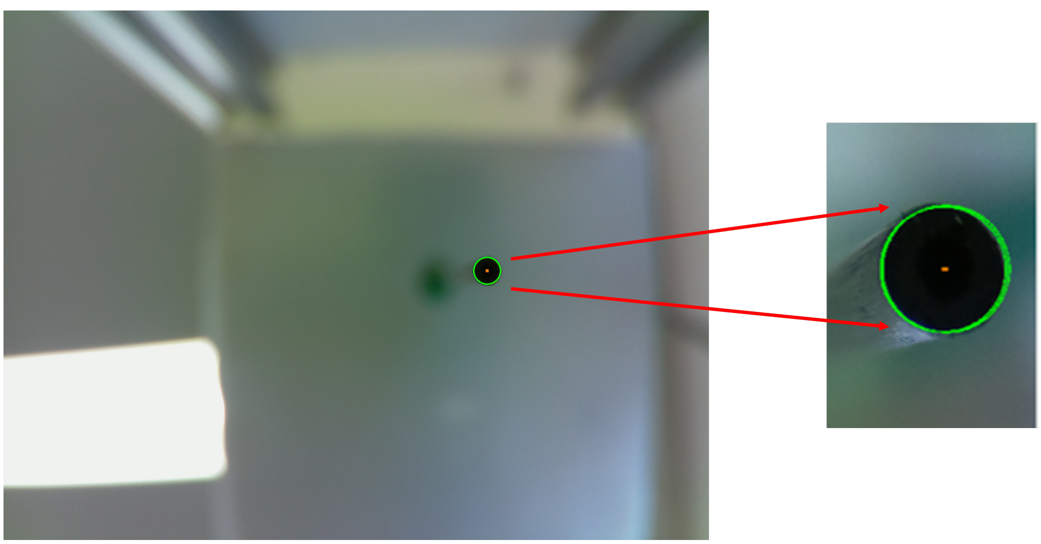

Fig 5 View from the digital camera on the Fermilab test stand and result of the HoughCircles algorithm. This picture shows a Tilting Spine with no optical fiber in at. The end of the spine appears as a dark disk, and the green circle around it and red dot on the pixel at its center are the results of the HoughCircles analysis. The individual pixels on the photo correspond to $\sim 4\mu m$ on a side. The single-pixel size limited the uncertainty in our spine position measurement with any particular setup.

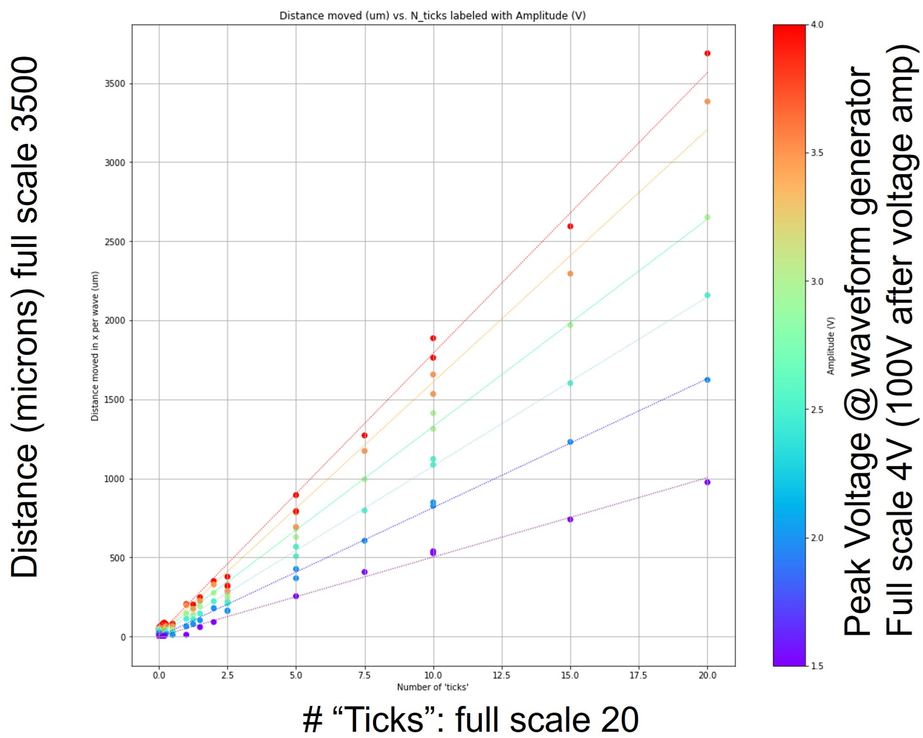

Fig 6 The movement of the tip of the FP (y-axis) versus number of ticks (x-axis) for 6 different sawtooth waveform amplitudes.

increases with increased sawtooth waveform amplitude. Then, armed with this information we experimented with various spine movement algorithms with the aim of achieving a 5 μm accuracy within 10 movements and determined how to move to any location.

On both test setups we positioned the spine iteratively, making a set of movements towards the desired location, followed by a position check using the camera, and then corrective movements as necessary. The algorithms were developed independently and seemed to depend on the performance of the waveform generators. At Fermilab we used a long, predetermined series of small steps to get into position. At U. Michigan the algorithm was to start with one or two big steps that made the maximum movement (250 μm for an 8V waveform generator pulse), then medium-sized, and lastly the smallest possible steps to get to within 5 μm of the desired position. Fig. 7 shows the movement steps for a randomly generated sequence of repositioning requests using the

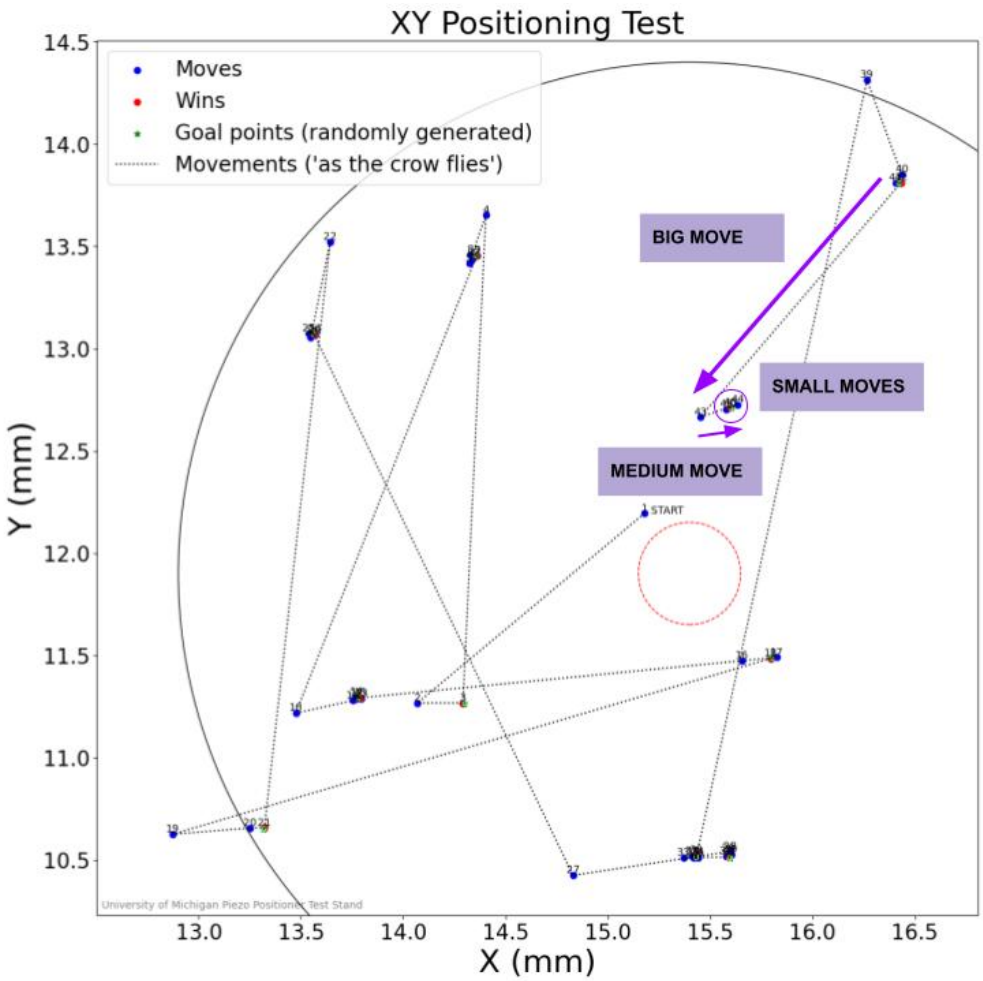

Fig 7 This shows a series of movements to randomly generated points within the patrol radius (shown) of our spine. These movements are carried out at the U. Michigan test stand, so the movement size is large at first and decreases as we close in on the desired position (win).

U. Michigan algorithm.

The digital cameras performed sufficiently well. The optics and geometry of the U. Michigan provided σ of $\sim 2\mu$m and a little better at the center of the imaged field. We didn't try to make corrections for imperfections, if any, in the camera optics, or for other systematic effects in our position measurements at the micron scale. The pixel scale using the Fermilab camera was set to about 4μm, just good enough to claim positioning success.

We performed systematic tests, repositioning the spine many times on a 1/2 mm grid within

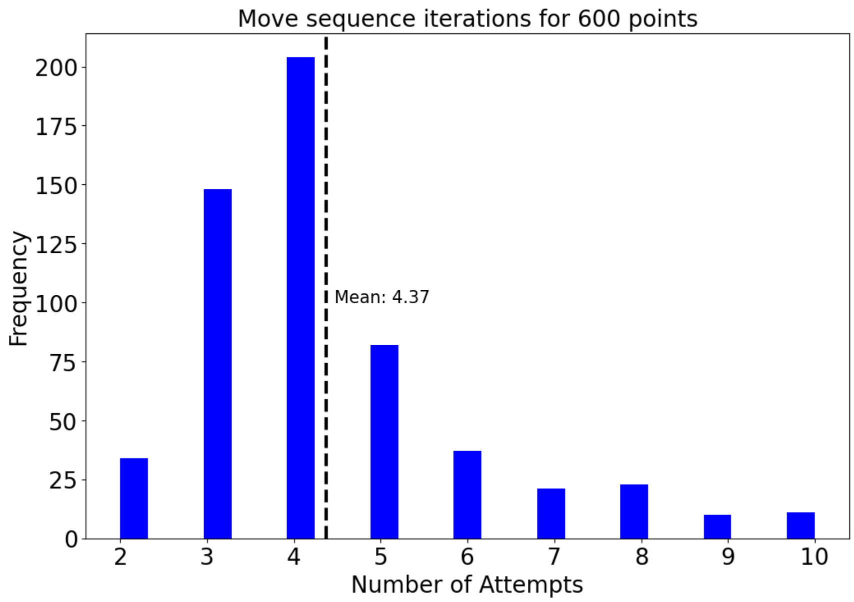

Fig 8 Histogram of the number of positioning attempts to reach targets on the 1/2 mm grid over the full patrol radius. The mode (mean) is 4 (4.37) iterations to position the spine within 5 microns of the desired location.

the patrol radius. With counted the number of movement iterations that it took to get within 5 microns of the desired location (bailing out after the 10th iteration) and the final location accuracy. These are shown in Fig.8 and Fig.9, respectively. These results are somewhat dependent on the movement algorithm, and we are showing results using the U. Michigan algorithm.

5 Summary and Discussion

The ambitions of near-term cosmology projects require the ability to provide spectroscopic redshifts of on order one billion targets. Accommodating 10,000 to 50,000 optical FPs will require either large focal surfaces (and therefore large and very expensive optical systems) or small pitch FPs.

In this note we described a simple unit Tilting Spine FP with a potential pitch of less than 6 mm (see Fig. 10), and a test stand, both built using off-the-shelf components and standard PYTHON software. We demonstrated basic functionality including the ability to be moved quickly and re-

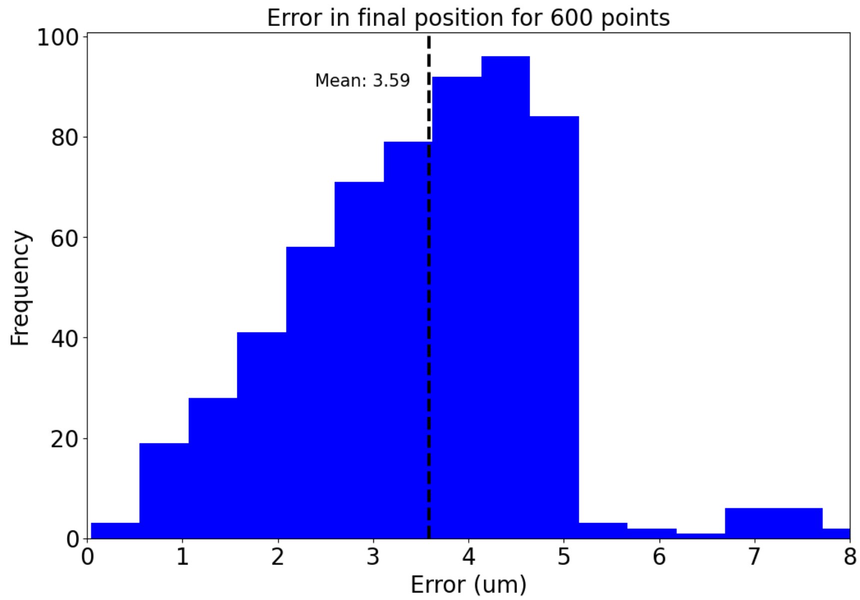

Fig 9 Histogram of positioning accuracy results during the 1/2 mm grid over the full patrol radius. There was a small handful of points with accuracy worse than 5 microns after the 10th iteration. The mean accuracy is 3.59 microns within the desired location, noting that we stopped moving if we were within 5 microns.

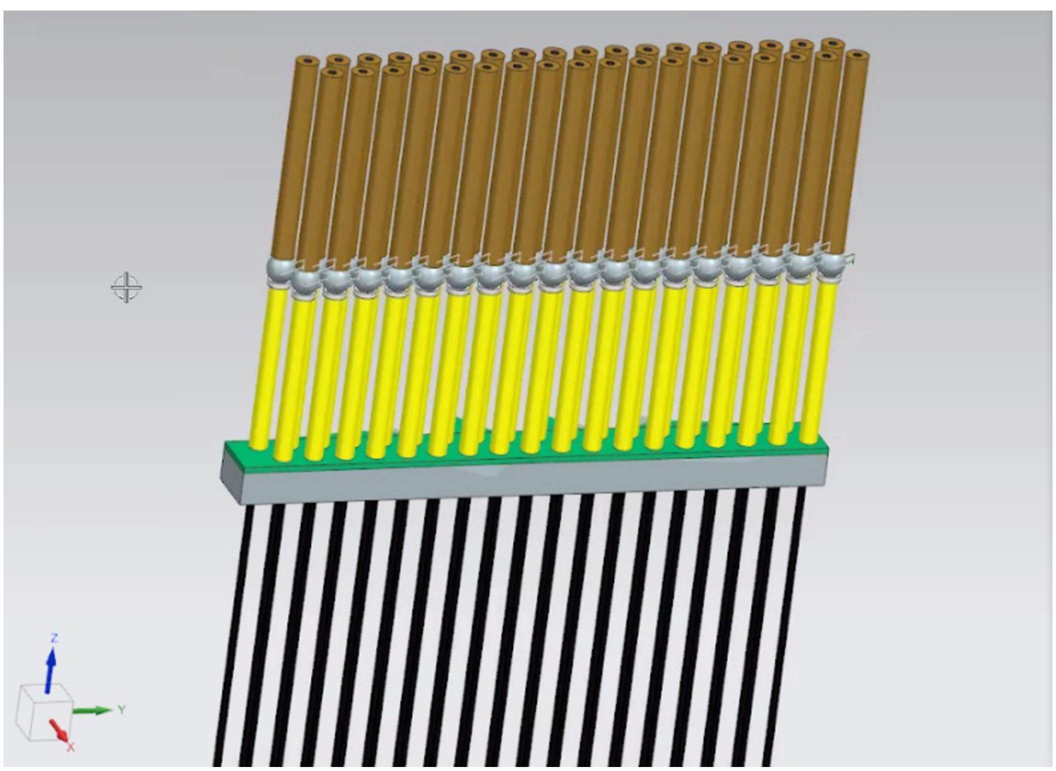

Fig 10 This cartoon shows what a small array of our simple FPs would look like with a 5.5 mm pitch. The two rows are offset by half the spacing. All the components would have to be smaller to achieve a further reduction in pitch

peatably into position with 5 μm precision. Our work has put us in a good position to explore both improvements to this simple FP that could arise from using customized components and to building and testing small arrays of FPs aimed at arriving at a practical instrument design.

Acknowledgements

The authors thank Jon Lawrence (Australian Astronomical Optical Research Centre at Macquarie University) for encouragement to perform this research, Andy Sheinis and Sam Barden (CFHT) for helpful discussions, and Paul Rubinov (Fermilab) for technical assistance. We hope to continue this effort and further our collaborative efforts. The work described in this manuscript was funded by Fermi Research Alliance, LLC under Contract No. DE-AC02-07CH11359 with the U.S. Department of Energy, Office of Science, Office of High Energy Physics through LDRD Project PPD-LDRD-2020.034.

References

1 The Sloan Digital Sky Survey, "SDSS." https://www.sdss4.org.

2 Abdurro'uf, K. Accetta, C. Aerts, *et al.*, "The Seventeenth Data Release of the Sloan Digital Sky Surveys: Complete Release of MaNGA, MaStar, and APOGEE-2 Data," *ApJS* **259**, 35 (2022).

3 K. Kuijken, C. Heymans, A. Dvornik, *et al.*, "The fourth data release of the Kilo-Degree Survey: ugri imaging and nine-band optical-IR photometry over 1000 square degrees," *A&A* **625**, A2 (2019).

4 Dark Energy Survey Collaboration, "The Dark Energy Survey Data Release 2," *ApJS* **255**, 20 (2021).

5 Dark Energy Survey Collaboration, "The Dark Energy Survey: more than dark energy – an overview," *MNRAS* **460**, 1270 (2016).

6 Dark Energy Survey Collaboration, "Dark Energy Survey Year 3 Results: Cosmological Constraints from Galaxy Clustering and Weak Lensing," *PRD* **105**, 023520 (2022).

7 Dark Energy Survey and Kilo-Degree Survey Collaborations, "DES Y3 + KiDS-1000: Consistent cosmology combining cosmic shear surveys," *Open Jour. Astrop.* **6**, (2023). https://doi:10.21105/astro.2305.17173.

8 Dark Energy Survey Collaboration, "The Complete Dark Energy Survey: Cosmological Constraints Using The Full 5-year Sample of Photometrically-Classified Type Ia Supernovae," *submitted to ApJ* , (2024). https://arxiv.org/abs/2401.02929.

9 P5 Committee, "Exploring the Quantum Universe: Pathways to Innovation and Discovery in Particle Physics," *Report of the 2023 Particle Physics Project Prioritization Panel* , (2023). https://www.usparticlephysics.org/wpcontent/uploads/2023/12/P5Report2023_120723-DRAFT_spreads.pdf.

10 D. J. Schlegel, S. Ferraro, G. Aldering, *et al.*, "A Spectroscopic Road Map for Cosmic Frontier: DESI, DESI-II, Stage-5." https://arxiv.org/abs/2209.03585v1.

11 K. Dawson, J. Frieman, K. Heitmann, *et al.*, "Cosmic visions dark energy: Small projects portfolio." https://arxiv.org/abs/1802.07216.

12 J. Annis, J. A. Newman, and A. Slosar, "Snowmass2021 Cosmic Frontier: Report of the CF04 Topical Group on Dark Energy and Cosmic Acceleration in the Modern Universe." https://arxiv.org/pdf/2209.08049.pdf (2022).

13 N. F. Staszak, J. Lawrence, D. M. Brown, *et al.*, "TAIPAN instrument fibre positioner and Starbug robots: engineering overview," *Proc. SPIE* **9912**, 99121W (2016).

14 N. Tamura, Y. Moritani, K. Yabe, *et al.*, "Prime Focus Spectrograph (PFS) for the Subaru Telescope: its start of the last development phase," *Proc. SPIE* **12184**, 1218410 (2022).

15 K. Fanning, R. Besuner, D. J. Eisenstein, *et al.*, "Overview and operation of the DESI focal plane," *Proc. SPIE* **12184**, 121847E (2022).

16 M. Akiyama, S. Smedley, P. Gillingham, *et al.*, "Performance of Echidna fiber positioner for FMOS on Subaru," *Proc. SPIE* **7018**, 70182V (2008).

17 R. Haynes, S. Barden, R. de Jong, *et al.*, "The 4MOST instrument concept overview," *Proc. SPIE* **9147**, 91476I (2014). https://doi.org/10.1117/12.2057253.

18 W. Saunders, G. Smith, J. Gilbert, *et al.*, "MOHAWK: a 4000-fiber positioner for DESpec," *Proc. SPIE* **8446**, 84464W (2012). https://doi.org/10.1117/12.925724.

19 R. Ellis, K. Dawson, J. Bland-Hawthorn, *et al.*, "SpecTel: A 10-12 meter class Spectroscopic Survey Telescope," , (2019). https://arxiv.org/abs/1907.06797.

20 A. Hill, K. Szeto, S. Barden, *et al.*, "MSE: Instrumentation for a massively multiplexed spectroscopic survey facility," *SPIE* **12184**, 121841B (2022).

21 G. Aldering, S. Bailey, C. Baltay, *et al.*, "The megamapper: A stage-5 spectroscopic instrument concept for the study of inflation and dark energy." https://arxiv.org/pdf/2209.04322.pdf.

22 K. Westfall, N. MacDonald, R. Kupke, *et al.*, "FOBOS: A next-generation spectroscopic facility." https://arXiv.org/abs/1907.07195.